





RESEARCH ARTICLE | FEBRUARY 15 2023

## Dynamics of chemical reactions on single nanocatalysts with heterogeneous active sites

Srabanti Chaudhury  ; Pankaj Jangid; Anatoly B. Kolomeisky  



*J. Chem. Phys.* 158, 074101 (2023)

<https://doi.org/10.1063/5.0137751>



View  
Online



Export  
Citation

CrossMark



**The Journal of Chemical Physics**  
**Special Topic: Adhesion and Friction**  
**Submit Today!**

# Dynamics of chemical reactions on single nanocatalysts with heterogeneous active sites

Cite as: *J. Chem. Phys.* **158**, 074101 (2023); doi: [10.1063/5.0137751](https://doi.org/10.1063/5.0137751)

Submitted: 5 December 2022 • Accepted: 30 January 2023 •

Published Online: 15 February 2023



View Online



Export Citation



CrossMark

Srabanti Chaudhury,<sup>1,a)</sup>  Pankaj Jangid,<sup>1</sup> and Anatoly B. Kolomeisky<sup>2,a)</sup> 

## AFFILIATIONS

<sup>1</sup> Department of Chemistry, Indian Institute of Science Education and Research, Dr. Homi Bhabha Road, Pune, Maharashtra 411008, India

<sup>2</sup> Department of Chemistry, Department of Physics and Astronomy, Department of Chemical and Biomolecular Engineering and Center for Theoretical Biological Physics, Rice University, Houston, Texas 77005-1892, USA

<sup>a)</sup> Authors to whom correspondence should be addressed: [srabanti@iiserpune.ac.in](mailto:srabanti@iiserpune.ac.in) and [tolya@rice.edu](mailto:tolya@rice.edu)

## ABSTRACT

Modern chemical science and industries critically depend on the application of various catalytic methods. However, the underlying molecular mechanisms of these processes still remain not fully understood. Recent experimental advances that produced highly-efficient nanoparticle catalysts allowed researchers to obtain more quantitative descriptions, opening the way to clarify the microscopic picture of catalysis. Stimulated by these developments, we present a minimal theoretical model that investigates the effect of heterogeneity in catalytic processes at the single-particle level. Using a discrete-state stochastic framework that accounts for the most relevant chemical transitions, we explicitly evaluated the dynamics of chemical reactions on single heterogeneous nanocatalysts with different types of active sites. It is found that the degree of stochastic noise in nanoparticle catalytic systems depends on several factors that include the heterogeneity of catalytic efficiencies of active sites and distinctions between chemical mechanisms on different active sites. The proposed theoretical approach provides a single-molecule view of heterogeneous catalysis and also suggests possible quantitative routes to clarify some important molecular details of nanocatalysts.

Published under an exclusive license by AIP Publishing. <https://doi.org/10.1063/5.0137751>

## I. INTRODUCTION

Catalysis is a set of physical-chemical processes that allow accelerating slow chemical reactions, and for this reason, it is an indispensable tool for synthetic chemical research as well as for a large number of industrial applications.<sup>1–5</sup> Nanocatalysts of different material compositions, such as metals, oxides, and sulfides, have wide applications ranging from chemical transformations to energy conversion and storage. There have been multiple investigations<sup>1,3,4,6,7</sup> to understand the molecular mechanism of chemical transformations in homogeneous and heterogeneous catalysis. Individual nanoparticles differ in size, shape, and surface sites, leading to time-dependent, particle-specific catalytic activity. Surface facets and surface defects on the surface can affect the catalytic activity. Surface structural dynamics can give rise to temporal activity fluctuations that also differ from one nanoparticle to another. So it is important to access individual nanoparticles to develop efficient catalysts. The ubiquitous heterogeneity among nanoparticles

makes it challenging to characterize the catalytic activity of nanoparticles. The majority of the studies are bulk investigations that provide only ensemble-averaged descriptions of catalyzed chemical reactions, missing out on these crucial molecular details of the catalytic processes.<sup>8</sup> Such ensemble measurements fail to capture the effects of their intrinsic heterogeneity that arise from their structural dispersion, heterogeneous surface sites, and surface restructuring dynamics. However, there is significant recent progress in resolving this problem due to developments of nanoparticle catalysts that could be quantitatively analyzed using a variety of single-molecule techniques, such as yielding important microscopic information on the molecular mechanisms of catalysis.<sup>9–14</sup>

Nanocatalysts have been known for more than 100 years, and they have been thoroughly investigated using multiple experimental and theoretical tools.<sup>2,5</sup> The mechanisms of heterogeneous catalysis are reasonably well understood at various levels. At the same time, recent experimental advances that provided single-molecule observations for these processes led to discoveries of new phenomena that

have not yet been addressed by theoretical studies.<sup>9,15</sup> It is important to develop a quantitative framework that would help to explain better these aspects of heterogeneous catalysis.

Single-molecule investigations of chemical reactions via fluorescence microscopy on nanocatalysts have uncovered multiple new features by measuring the dynamics with unprecedented spatial and temporal resolutions.<sup>9,10</sup> Single-molecule microscopy of fluorogenic reactions was initially developed for studying catalysis by single enzyme molecules.<sup>16,17</sup> In 2006, this approach was applied for the first time to investigate heterogeneous catalysis on layered hydroxide microcrystals<sup>18</sup> and photocatalysis on TiO<sub>2</sub> films,<sup>19</sup> and it was later extended to study catalysis on single metal nanoparticles.<sup>10</sup> These studies clarified the microscopic mechanisms of chemical processes for several systems that could not be obtained by ensemble-averaged methods.<sup>9,10</sup> In the context of single nanocatalysts, one of the main results was a very large heterogeneity and strong stochastic fluctuations in the dynamic properties of catalyzed chemical reactions.<sup>9,10,15,20</sup> Experiments on single nanocatalysts exhibited very broad distributions of effective rates for the formation and release of the products of chemical reactions, as well as the dependence of catalytic activities on the sizes of nanoparticles. It was found that there are several different types of active sites on the same nanoparticles that lead to the same products but differ in their catalytic efficiency.<sup>15</sup> Site-specific catalytic activity was also reported in catalytic reactions on two types of shaped nanocrystals: Au nanorods and nanoplates. It was found that for 1D nanocrystals such as Au nanorods, the catalytic activity at different locations within the same surface facets on a single nanorod is not constant.<sup>21</sup> These findings emphasized the importance of surface defects and other heterogeneities. Several possible reasons for all these observations have been identified. The surfaces of nanoparticles might undergo a dynamic restructuring that results in fluctuations in the catalytic activity.<sup>1,7,22,23</sup> The dynamic surface restructuring is also found to be slower for larger nanoparticles, and this might partially explain the size dependence of the transition rates for chemical reactions on nanocatalysts.<sup>24</sup> Meanwhile, the microscopic origin of stochastic fluctuations in the catalytic properties of nanoparticles has been identified,<sup>15,21,24,25</sup> currently, there is no theoretical framework to quantitatively account for the effects of heterogeneity at the single-particle level, which could also provide more information on the molecular mechanisms of catalytic processes.

Single-molecule investigations of chemical reactions on nanocatalysts stimulated significant theoretical efforts to better describe the microscopic picture of catalysis. The size-dependent catalytic activity of gold (Au) clusters at the single-cluster level has been studied using the Langmuir–Hinshelwood mechanism and density functional theory calculations. The size-dependent electronic structure of Au clusters is responsible for this size effect on the catalytic product formation and dissociation processes.<sup>26</sup> However, because the sizes of catalytic nanoparticles utilized in these experiments are still quite large (ranging from ~100 nm up to several microns),<sup>9</sup> various computer simulation methods and numerical methods, such as Carr–Parrinello molecular dynamics simulations and quantum-chemical calculations, could not be used to understand the dynamics of catalytic processes, indicating that mesoscopic theoretical methods had to be employed. Initially, these processes have been analyzed using a simplified mean-field Langmuir–Hinshelwood approach that assumed that there is

one “effective” catalytic site that represents all active sites in the nanoparticle.<sup>27</sup> However, this theoretical method could not explain some important features, such as the size-dependent catalytic activity, that have been observed experimentally. A more advanced approach is based on the theory of first-passage processes to explain the dynamics of catalytic processes, and it accounts for several properties, including the number of active sites and the role of stochasticity.<sup>28,29</sup> This method, however, neglected the molecular details of the chemical reactions, and for this reason, it could not be utilized to better understand the microscopic origin of the catalytic effect.

We recently developed a new theoretical framework based on discrete-state chemical-kinetic analysis that takes into account the stochasticity of individual chemical reactions at each catalytic site on a single nanoparticle.<sup>30,31</sup> The advantage of this stochastic approach is that all dynamic properties of chemical processes on single nanocatalysts can be explicitly evaluated. This allowed us to clarify several important aspects of catalysis on nanoparticles by linking theoretical predictions with available experimental observations.<sup>30,31</sup> However, the assumption that all active sites are identical in their catalytic efficiency is unrealistic and may fail to explain the following experimental findings. Temporal catalytic dynamics of single gold nanoparticles in single molecule fluorescence microscopy measurements revealed that there are two types of surface sites with different catalytic activities.<sup>15</sup> Single molecule imaging and kinetic studies provide evidence of the crystal-face dependency of the TiO<sub>2</sub> photocatalytic reactions.<sup>32</sup> The catalytic kinetics and dynamics of the different types of surface atoms on metal nanocatalysts were studied quantitatively using single-molecule nanocatalysis of Pd nanocrystals. The results showed that the different types of surface atoms (plane or edge) on Pd nanocubes lead to different product dissociation kinetics.<sup>33</sup> All these observations explain the need to build up a theoretical approach that allows for quantitative investigation of the role of heterogeneity in catalytic processes on nanoparticles.

In this paper, we present a minimal model by extending the original discrete-state chemical-kinetic method to take into account the possibility of different active sites with different mechanisms for catalyzed chemical reactions. Using the stationary-state calculations and the first-passage analysis, the dynamic properties of chemical processes on single nanocatalysts are explicitly evaluated for the simplest heterogeneous system with only two types of active sites. Several different sources of heterogeneity are identified and fully quantified. It is argued that the application of the proposed theoretical approach to real nanocatalyst systems could uncover some important molecular details of the underlying chemical processes.

The paper is organized in the following way. Our theoretical method is described in Sec. II. The specific results are given and discussed in Sec. III. Section IV summarizes and concludes our results.

## II. THEORETICAL MODEL

To understand better our theoretical method, it is important to briefly describe the details of single-molecule measurements of chemical processes on nanocatalysts.<sup>9,10</sup> In those experiments, the catalyzed chemical reactions yield products that are fluorescent and can be studied at the single-particle level. More specifically, times

between fluorescence signals from single active site reactions are accurately measured for different spatial locations on the nanoparticle, and these time trajectories are then statistically analyzed. The goal of our theoretical approach is to provide a quantitative framework that connects these measurements with underlying microscopic details for nanocatalysts.

Now, to quantify the effect of heterogeneity on the dynamic properties of catalyzed chemical reactions, we consider a minimal theoretical model with a single nanocatalyst that has  $N$  active sites, as illustrated in Fig. 1(a). There are two types of active sites, denoted as  $R_1$  and  $R_2$ , that catalyze the chemical reactions to produce the same products but with different molecular mechanisms [see Fig. 1(b)]. The number of sites that follow the mechanism  $R_1$  is equal to  $N_1$ , and the number of sites that follow the mechanism  $R_2$  is equal to  $N_2$ . The total number of active sites per nanoparticle is  $N_1 + N_2 = N$ . To simplify the analysis, we assume that the mechanism  $R_1$  is a set of sequential irreversible transitions between  $M_1$  intermediate states with all rates equal to  $a_1$  [Fig. 1(b)]. In this mechanism,  $C$  corresponds to the empty state of the catalyst,  $S$  is the substrate, and  $CS_j^{(1)}$  ( $j = 1, \dots, M_1$ ) are intermediate states with the bound substrate in different chemical conformations on the path to the product.

Similarly, the mechanism  $R_2$  is viewed as a set of sequential irreversible transitions between  $M_2$  intermediate states with all rates equal to  $a_2$ . Here, we label the intermediate states as  $CS_j^{(2)}$  with  $j = 1, \dots, M_2$  [see Fig. 1(b)]. It has been argued before that using more realistic reversible transitions with different rates will not change the microscopic picture of processes on the nanocatalyst, justifying our simplified theoretical model with irreversible transitions.<sup>31</sup> We also tested this assumption in Monte Carlo simulations (results are not shown). Using more realistic reversible transition rates will change the quantitative estimates of dynamic properties, but the main physical predictions obtained in this work are still valid. Therefore, we can use the simplified model in Fig. 1 to understand the role of heterogeneity in nanocatalysts.

It should be noted that in our theoretical model, it is assumed that the catalytic activities of reactive sites are constant and do not change with time. However, there are experimental observations and theoretical calculations suggesting that due to the dynamic restructuring of nanoparticle surfaces, the catalytic efficiencies of active sites might fluctuate with time.<sup>34,35</sup> Since we are calculating the stationary dynamic properties of chemical reactions on nanocatalysts, our theoretical picture can be viewed as a mean-field approach

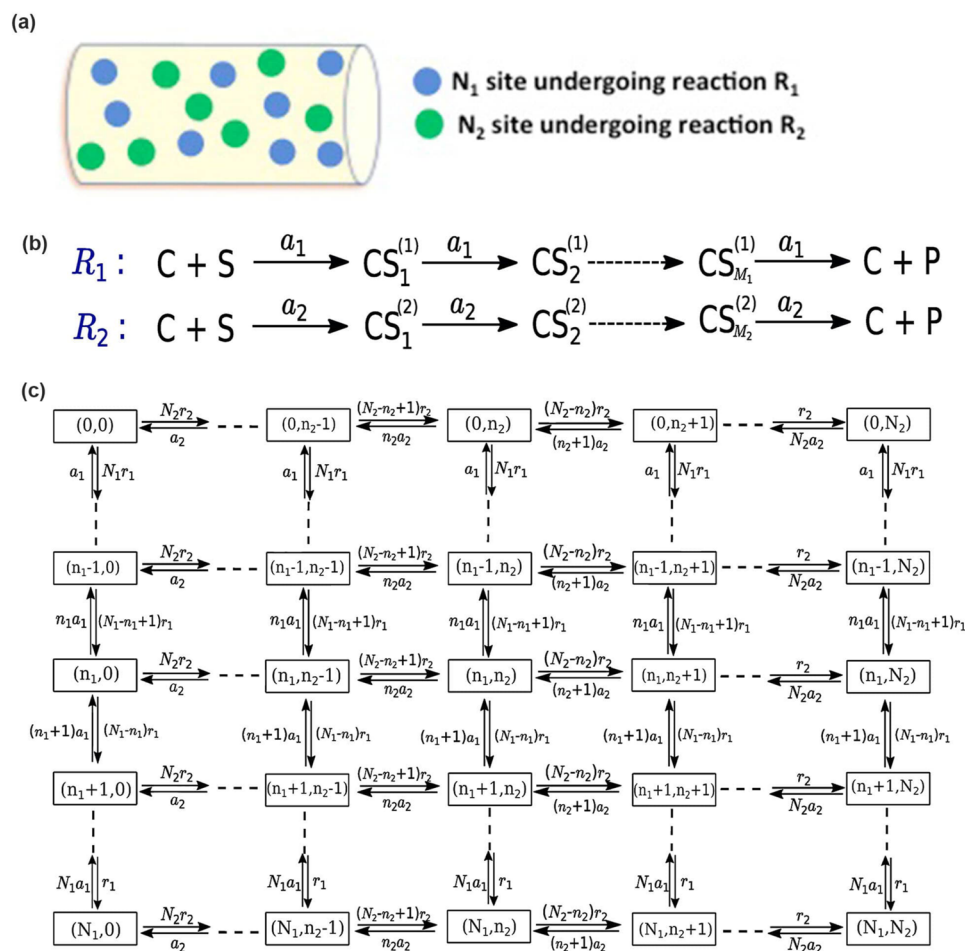


**FIG. 1.** A schematic representation of chemical processes on a single nanocatalyst with two different types of active sites. (a) Catalytic nanoparticle is viewed as a nanorod with two types of active sites. There are  $N_1$  sites where the chemical reaction  $R_1$  is taking place and  $N_2$  sites where the chemical mechanism  $R_2$  is taking place. (b) Chemical mechanisms on different active sites: sequential chemical reactions with  $M_1$  intermediates for the mechanism  $R_1$  and sequential chemical reactions with  $M_2$  intermediates for the mechanism  $R_2$ . (c) Effective chemical-kinetic scheme for chemical processes on the single nanocatalyst. Each discrete state  $(n_1, n_2)$  corresponds to the state of the system with  $n_1$  ( $0 \leq n_1 \leq N_1$ ) active sites in the chemical conformation  $CS_{M_1}^{(1)}$  and  $n_2$  ( $0 \leq n_2 \leq N_2$ ) active sites in the state  $CS_{M_2}^{(2)}$  just before making the product.

with the average activities assigned to each type of catalytic site. These arguments significantly simplify the calculations of dynamic properties.

Another important assumption in our theoretical approach is the independence of active sites from each other, i.e., chemical reactions can happen independently at each site. Meanwhile, this might be a reasonable approximation for some systems with a low density of catalytic sites, recent experimental studies on single nanocatalysts have discovered cooperativity between the activities of neighboring sites.<sup>36</sup> At the same time, the amplitudes of such correlations seem to be relatively small.<sup>36</sup> In addition, a discrete-state stochastic analysis similar to what is presented in this work has already been explored to analyze the catalytic cooperativity in nanoparticles.<sup>37</sup> The results obtained in these studies support the use of the independence assumption in our theoretical analysis.

To comprehensively describe all processes that are taking place on the single nanocatalyst, we construct an effective chemical-kinetic scheme as presented in Fig. 1(c). Our idea is to identify different effective states of the system by counting how many of the active sites are in conformations  $CS_{M_1}^{(1)}$  or  $CS_{M_2}^{(2)}$ , i.e., when the active sites are in the chemical conformations just before the product is made.<sup>30,31</sup> This is stimulated by the nature of single-molecule experiments on nanocatalysts, in which the signal that the reaction occurs comes only after the product molecule is created.<sup>9</sup> Following this idea, we define a generic stochastic state of the nanocatalyst as  $(n_1, n_2)$ , which corresponds to having exactly  $n_1$  ( $0 \leq n_1 \leq N_1$ ) active sites of the type  $R_1$  in the conformation  $CS_{M_1}^{(1)}$  and  $n_2$  ( $0 \leq n_2 \leq N_2$ ) active sites of the type  $R_2$  in the conformation  $CS_{M_2}^{(2)}$ .

From the state  $(n_1, n_2)$ , the system can transition into the state  $(n_1 - 1, n_2)$  with a rate  $n_1 a_1$  [upside transitions in the scheme in Fig. 1(c)]. This is because the product can be made at  $n_1$  sites with the rate  $a_1$ , and all sites are independent of each other. Similarly, from the state  $(n_1, n_2)$ , the system can transition into the state  $(n_1, n_2 - 1)$  with a rate  $n_2 a_2$  [left-direction transitions in the scheme in Fig. 1(c)] because originally there are  $n_2$  active sites from which the product can be made with the rate  $a_2$  at each site. From the state  $(n_1, n_2)$ , the system can also move into the state  $(n_1 + 1, n_2)$  with a rate  $(N_1 - n_1) r_1$  [downside transitions in Fig. 1(c)], where the effective rate constant  $r_1$  is given by

$$r_1 = \frac{a_1}{M_1}. \quad (1)$$

It can be explained by noting that this transition corresponds to an increase of one in the number of active sites of type  $R_1$  in the conformation  $CS_{M_1}^{(1)}$ . There are  $(N_1 - n_1)$  active sites of the type  $R_1$  that are not in the final conformation before making the product. This reaction can happen with the rate  $a_1$  only from the conformation  $CS_{M_1-1}^{(1)}$ , but because all transition rates in the chemical mechanism  $R_1$  are the same, the probability to encounter this conformation is equal to  $1/M_1$ . It should be noted that we assume here that the system is already in a stationary state and that the uniform distributions for individual conformations are already achieved. Similar arguments suggest that transitions that lead from the state  $(n_1, n_2)$  to the state  $(n_1, n_2 + 1)$  [right-direction transitions in the scheme in Fig. 1(c)] are taking place with a rate  $(N_2 - n_2) r_2$ , where

$$r_2 = \frac{a_2}{M_2}. \quad (2)$$

Calculations of dynamic properties for the discrete-state stochastic scheme in Fig. 1(c) can be performed using different approaches, but here we chose the method of first-passage probabilities.<sup>38–41</sup> This is especially convenient for our system since in the single-molecule experiments on nanoparticles, the catalytic events are counted as soon as the product molecules appear for the first time at active sites, which is measured, for example, by changes in the fluorescence signals.<sup>9</sup> In this approach, we define  $F_{n_1, n_2}(t)$  as a probability density function to complete a catalytic cycle and to make the product  $P$  for the first time at time  $t$  if, at  $t = 0$ , the system started in the stochastic state  $(n_1, n_2)$ . The time evolution of these functions is governed by a set of backward master equations,

$$\begin{aligned} \frac{dF_{0,0}(t)}{dt} &= N_1 r_1 F_{1,0}(t) + N_2 r_2 F_{0,1}(t) - (N_1 r_1 + N_2 r_2) F_{0,0}(t), \\ \frac{dF_{1,0}(t)}{dt} &= (N_1 - 1) r_1 F_{2,0}(t) + N_2 r_2 F_{1,1}(t) + a_1 F_{P,0}(t) \\ &\quad - [(N_1 - 1) r_1 + N_2 r_2] F_{1,0}(t), \\ \frac{dF_{0,1}(t)}{dt} &= N_1 r_1 F_{1,1}(t) + (N_2 - 1) r_2 F_{0,2}(t) + a_2 F_{0,P}(t) \\ &\quad - [N_1 r_1 + (N_2 - 1) r_2] F_{0,1}(t), \\ &\vdots \\ \frac{dF_{n_1, n_2}(t)}{dt} &= (N_1 - n_1) r_1 F_{n_1+1, n_2}(t) + (N_2 - n_2) r_2 F_{n_1, n_2+1}(t) \\ &\quad + n_1 a_1 F_{P, n_2}(t) + n_2 a_2 F_{n_1, P}(t) - [(N_1 - n_1) r_1 \\ &\quad + (N_2 - n_2) r_2 + n_1 a_1 + n_2 a_2] F_{n_1, n_2}(t), \\ &\vdots \\ \frac{dF_{N_1, N_2}(t)}{dt} &= N_1 a_1 F_{P, N_2}(t) + N_2 a_2 F_{N_1, P}(t) \\ &\quad - [N_1 a_1 + N_2 a_2] F_{N_1, N_2}(t), \end{aligned} \quad (3)$$

where  $F_{P, n_2}(t)$  and  $F_{n_1, P}(t)$  are the first-passage probability density functions for the product states with molecules  $P$  just created with  $n_1$  molecules in the state  $R_1$  and  $n_2$  molecules in the state  $R_2$ , respectively. One can estimate these functions as  $F_{P, n_2}(t) = F_{n_1, P}(t) = \delta(t)$ . This physically means that if the system starts in such product states, the process is immediately accomplished.

As explained in the supplementary material, the set of backward master equations in Eq. (3) can be explicitly solved using Laplace transformations of the first-passage probability density functions,

$$\tilde{F}_{n_1, n_2}(s) = \int_0^\infty e^{-st} F_{n_1, n_2}(t) dt. \quad (4)$$

It leads to the following equations:

$$\begin{aligned} \tilde{F}_{n_1, n_2}(s) &= X(n_1, n_2) + \sum_{k=1}^{N_2 - n_2} \sum_{i_1=n_1}^{N_1} \sum_{i_2=i_1}^{N_1} \sum_{i_3=i_2}^{N_1} \cdots \sum_{i_k=i_{k-1}}^{N_1} X(i_k, n_2 + k) \\ &\quad \times \prod_{p=1}^k Q(i_p, n_2 + p - 1), \end{aligned} \quad (5)$$

where the explicit expressions for the auxiliary functions  $X(n_1, n_2)$  and  $Q(i, j)$  are given in the supplementary material [see Eqs. (9) and (10) there]. This allows us to evaluate all the dynamic properties

of the system. For example, the mean first-passage times  $\langle T_{n_1, n_2} \rangle$ , and the mean squared first-passage times,  $\langle T_{n_1, n_2}^2 \rangle$ , to complete the chemical reaction starting from the stochastic state  $(n_1, n_2)$  can be estimated using

$$\langle T_{n_1, n_2} \rangle \equiv \int_0^\infty t F_{n_1, n_2}(t) dt = - \left( \frac{\partial \tilde{F}_{n_1, n_2}(s)}{\partial s} \right)_{s=0} \quad (6)$$

and

$$\langle T_{n_1, n_2}^2 \rangle \equiv \int_0^\infty t^2 F_{n_1, n_2}(t) dt = \left( \frac{\partial^2 \tilde{F}_{n_1, n_2}(s)}{\partial s^2} \right)_{s=0}. \quad (7)$$

Other dynamic features of the chemical processes on single nanocatalysts can be evaluated in a similar fashion.

### III. RESULTS AND DISCUSSIONS

#### A. Distributions of different states of the nanocatalyst

Equations (6) and (7) describe the dynamic properties of the system if the catalyzed chemical reactions initiate *exactly* from the state  $(n_1, n_2)$ . However, the catalytic process can start from any of the  $[(N_1 + 1)(N_2 + 1) - 1]$  discrete states; see Fig. 1(c), and note that it cannot start from the state  $(N_1, N_2)$  since in this state there are no empty sites for the substrate to bind. To describe the reaction dynamics for the single catalyst, as measured in the single-molecule experiments, one should average over all possible initial states of the system. To do so, we define  $P_{n_1, n_2}(N_1, N_2, t)$  as the probability of finding the nanocatalyst with  $N_1$  active sites of type  $R_1$  and  $N_2$  active sites of type  $R_2$  in the effective state  $(n_1, n_2)$  at time  $t$ . At large times,  $t \rightarrow \infty$ , the system is expected to reach stationary conditions, allowing us to estimate the steady-state probabilities  $P_{n_1, n_2}(N_1, N_2)$  via forward master equations, as explained in detail in the [supplementary material](#). This leads to the following expressions:

$$P_{n_1, n_2}(N_1, N_2) = \frac{\binom{N_1}{n_1} \left(\frac{1}{M_1}\right)^{n_1} \binom{N_2}{n_2} \left(\frac{1}{M_2}\right)^{n_2}}{\left(1 + \frac{1}{M_1}\right)^{N_1} \left(1 + \frac{1}{M_2}\right)^{N_2}}, \quad (8)$$

with  $\binom{N}{n} = \frac{N!}{(N-n)!n!}$  being a binomial coefficient. This equation can also be rewritten as

$$P_{n_1, n_2}(N_1, N_2) = \frac{\binom{N_1}{n_1} x_1^{n_1} \binom{N_2}{n_2} x_2^{n_2}}{(1 + x_1)^{N_1} (1 + x_2)^{N_2}}, \quad (9)$$

where  $x_1 = 1/M_1$  and  $x_2 = 1/M_2$ .

#### B. Evaluation of reaction times

Now, the mean reaction times  $\langle \tau \rangle_{N_1, N_2}$  for the single nanocatalyst with  $N_1$  sites of the type  $R_1$  and  $N_2$  sites of the type  $R_2$ , which are equivalent to experimentally measured catalytic turnover times, can be explicitly computed. This can be done by averaging over all states from which the catalyzed reactions initiate,

$$\langle \tau \rangle_{N_1, N_2} = \sum_{n_1=0}^{N_1} \sum_{n_2=0}^{N_2} f(n_1, n_2) \langle T_{n_1, n_2} \rangle, \quad (10)$$

where the coefficient  $f(n_1, n_2)$  gives the probability for the catalytic cycle to start in the effective state  $(n_1, n_2)$ . Similar calculations can be done for the mean-squared reaction times,

$$\langle \tau^2 \rangle_{N_1, N_2} = \sum_{n_1=0}^{N_1} \sum_{n_2=0}^{N_2} f(n_1, n_2) \langle T_{n_1, n_2}^2 \rangle. \quad (11)$$

The probability factor  $f(n_1, n_2)$  reflects the number of sites in the state  $(n_1, n_2)$  from which the catalyzed reaction might start. Since  $n_1$  sites of the type  $R_1$  and  $n_2$  sites of the type  $R_2$  are already in conformations before the final product is made, there are only  $(N_1 - n_1)$  sites of the type  $R_1$  and  $(N_2 - n_2)$  sites of the type  $R_2$  where the catalytic process might initiate. One should also notice that the probability to start the catalytic cycle on the sites of type  $R_1$  is proportional to  $r_1$ , while the probability to start on the sites of type  $R_2$  is proportional to  $r_2$ . This suggests that these factors can be evaluated using

$$f(n_1, n_2) = \frac{[(N_1 - n_1)r_1 + (N_2 - n_2)r_2]P_{n_1, n_2}(N_1, N_2)}{\sum_{n_1=0}^{N_1} \sum_{n_2=0}^{N_2} [(N_1 - n_1)r_1 + (N_2 - n_2)r_2]P_{n_1, n_2}(N_1, N_2)}, \quad (12)$$

which using Eq. (9) and the properties of binomial coefficients can be rewritten in a simpler form,

$$f(n_1, n_2) = \frac{\frac{N_1 a_1 x_1}{1+x_1} P_{n_1, n_2}(N_1 - 1, N_2)}{\frac{N_1 a_1 x_1}{1+x_1} + \frac{N_2 a_2 x_2}{1+x_2}} + \frac{\frac{N_2 a_2 x_2}{1+x_2} P_{n_1, n_2}(N_1, N_2 - 1)}{\frac{N_1 a_1 x_1}{1+x_1} + \frac{N_2 a_2 x_2}{1+x_2}}. \quad (13)$$

Note also that  $f(N_1, N_2) = 0$  since the catalytic cycle can never start from this effective state. It is important to note that the factor  $f(n_1, n_2)$  reflects the relative probability of where the reaction might start next for the given overall state of the system and is not the same as the stationary probability of different states that only specifies the current situation of the system.

The mean reaction times can now be explicitly calculated using Eq. (10). However, here we would like to show a simpler alternative way to estimate this quantity. The stationary flux to make the product molecules starting from the state  $(n_1, n_2)$  is equal to

$$J_{n_1, n_2} = (n_1 a_1 + n_2 a_2) P_{n_1, n_2}(N_1, N_2). \quad (14)$$

In this equation, the coefficient  $(n_1 a_1 + n_2 a_2)$  reflects the fact that there are  $n_1$  sites of the type  $R_1$  that are ready to form the product with the rate  $a_1$  and  $n_2$  sites of the type  $R_2$  that are ready to form the product with the rate  $a_2$ . Then the overall stationary reaction flux from the single nanocatalyst is given by

$$J = \sum_{n_1=0}^{N_1} \sum_{n_2=0}^{N_2} J_{n_1, n_2} = \frac{N_1 a_1}{1 + M_1} + \frac{N_2 a_2}{1 + M_2}, \quad (15)$$

which is obtained by substituting the expressions for  $P_{n_1, n_2}$  into Eq. (14) and summing over all possible values of  $n_1$  and  $n_2$ . Importantly, the reciprocal of this quantity is exactly equal to the mean reaction time,

$$\langle \tau \rangle_{N_1, N_2} = \frac{1}{J} = \frac{1}{\frac{N_1 a_1}{1 + M_1} + \frac{N_2 a_2}{1 + M_2}}. \quad (16)$$

For the same number of intermediates involved in both reaction mechanisms  $R_1$  and  $R_2$ , i.e., when  $M_1 = M_2 = M$ , the mean reaction time simplifies further into

$$\langle \tau \rangle_{N_1, N_2} = \frac{1 + M}{N_1 a_1 + N_2 a_2}. \quad (17)$$

The results of theoretical calculations for mean reaction times on single nanocatalysts with two types of active sites are presented in Fig. 2. As expected, the mean reaction times decrease for larger numbers of active sites as more chemical reactions can take place at them, lowering the time intervals between the appearance of product molecules. In agreement with these arguments, increasing the transition rates ( $a_1$  or  $a_2$ ) also lowers the mean reaction times [see Fig. 2(a), where  $a_1$  is varied]. In addition, increasing the number of intermediate states in each chemical mechanism slows down the overall process since it takes longer to reach the final product, and this fully agrees with the observations in Fig. 2(b). Here it is also shown that keeping the number of active sites fixed while increasing the fraction of sites where reactions are taking place faster [a larger  $N_2$  in Fig. 2(b)] also lowers the mean reaction times, as expected.

### C. Analysis of stochastic fluctuations

It has been argued before that to understand the mechanisms of catalytic processes on single nanocatalysts, it is important to consider a dimensionless parameter  $R$ , called *randomness*,<sup>30,31</sup> which is defined as<sup>42</sup>

$$R = \frac{\langle \tau^2 \rangle_{N_1, N_2} - \langle \tau \rangle_{N_1, N_2}^2}{\langle \tau \rangle_{N_1, N_2}^2}. \quad (18)$$

It provides a convenient measure of the degree of stochastic fluctuations for chemical reactions on nanocatalysts. Since a single-step Poisson process is expected to have  $R = 1$ , deviations from unity serve as an indicator of the amplitude of temporal fluctuations in

dynamic properties and heterogeneity in the system. Smaller values of the randomness parameter correspond to larger stochastic fluctuations and larger heterogeneity. One can think of the quantity  $1/R$  as an estimate for the number of rate-limiting transitions in the system. Clearly, the larger this number ( $1/R$ ), the more stochastic fluctuations are observed in the system.

Using Eqs. (10) and (11), the randomness parameter can be explicitly evaluated for all possible parameters of the nanocatalyst. The results presented in Fig. 3 show the randomness  $R$  as a function of the number of active sites  $N_1$  if the total number of active sites is fixed. In all cases, the non-monotonic dependence is observed, suggesting that there are specific values of  $N_1$  at which the system exhibits a maximal possible degree of stochastic fluctuations. Interestingly, this number depends on the transition rates  $a_1$  [Fig. 3(a)] and  $a_2$  [Fig. 3(b)]. To explain these observations, we notice that the maximal degree of stochastic fluctuations is expected when the contributions from the reaction sites of types  $R_1$  and  $R_2$  are comparable, i.e., the corresponding fluxes are of the same magnitude,

$$J_1 = \frac{N_1 a_1}{1 + M_1} \simeq J_2 = \frac{N_2 a_2}{1 + M_2}. \quad (19)$$

Then, we estimate that the minimal value of the randomness parameter (maximal randomness) can be achieved when

$$N_1 \simeq \frac{N a_2}{\left(\frac{1+M_2}{1+M_1}\right) a_1 + a_2}. \quad (20)$$

For  $M_1 = M_2 = M$ , this result simplifies into

$$N_1 \simeq \frac{N a_2}{a_1 + a_2}. \quad (21)$$

One can easily check that these arguments perfectly explain the non-monotonic behavior of the randomness parameter and the location of the corresponding minima in Fig. 3.

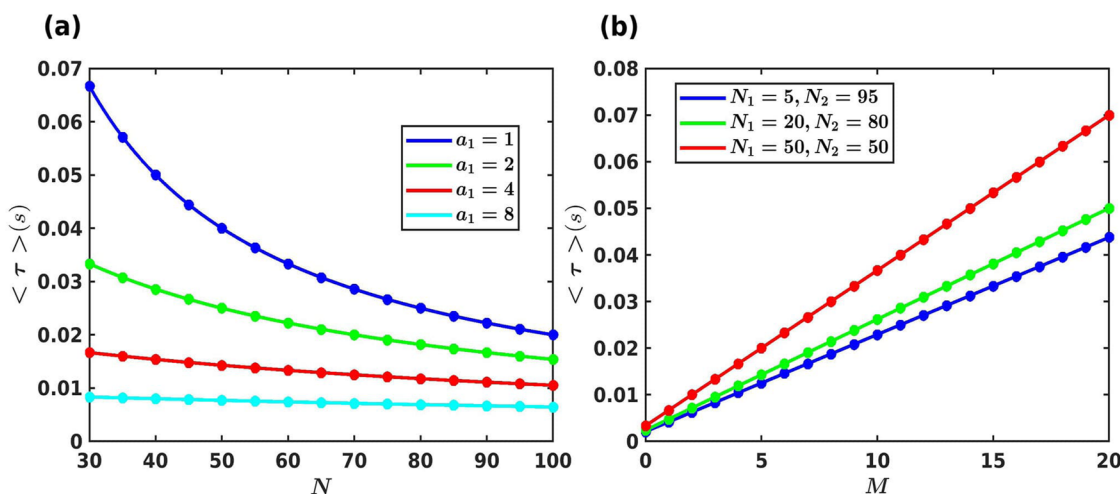


**FIG. 2.** Mean reaction times (a) as a function of the total number of active sites  $N$  on the single nanocatalyst with  $N_1 = 30$  for different transition rates  $a_1$  with  $M_1 = M_2 = 1$  and  $a_2 = 1$ ; (b) as a function of the number of intermediate states  $M_1 = M_2 = M$  for a different number of active sites  $N_1$  with  $a_1 = 1$  and  $a_2 = 5$ , and with the total number of active sites equal to  $N = 100$ . The curves are analytical predictions [using Eqs. (16) and (17)], and the symbols are from Monte Carlo computer simulations.

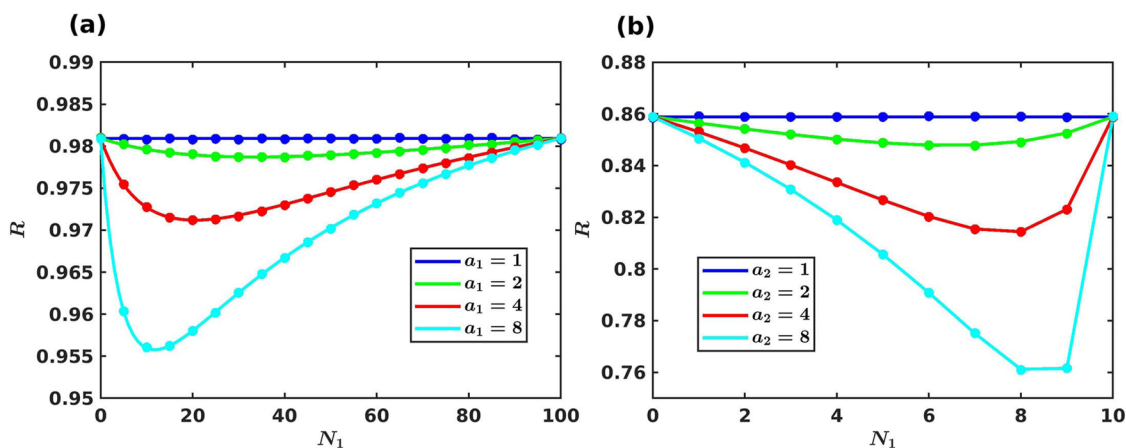


**FIG. 3.** Randomness parameter as a function of the number  $N_1$  of the active sites of type  $R_1$  for different catalytic activities specified by  $a_1$  and  $a_2$  with  $M_1 = M_2 = 1$ . Calculations are performed for (a)  $N = 100$  and  $a_2 = 1$ , and (b)  $N = 10$  and  $a_1 = 1$ . The curves are analytical predictions [using Eq. (18)], and the symbols are from Monte Carlo computer simulations.

The results of our theoretical calculations also indicate that for the fixed number of active sites  $N_1$  and  $N_2$ , increasing the catalytic activity [larger transition rates  $a_1$  in Fig. 3(a) or larger transition rates  $a_2$  in Fig. 3(b)] always lowers the randomness parameter. This corresponds to larger degrees of stochastic fluctuations in the system. In addition, one could see that decreasing the number of active sites [ $N = 10$  in Fig. 3(b) vs  $N = 100$  in Fig. 3(a)] lowers the randomness. This is a consequence of the fact that when there are only a few active sites, the stochastic effects are very pronounced, while for large  $N$ , the stochasticity starts to average out.

#### D. Analysis of different sources of heterogeneity

The results presented in Fig. 3 are also convenient for analyzing the different sources of heterogeneity in chemical reactions on single nanocatalysts. In this system, we identify three different sources of heterogeneity that influence the overall level of stochastic fluctuations. First, the stochastic nature of the chemical reactions themselves leads to the fluctuations; one can see from Fig. 3 that for  $N_1 = 0$  when there is only one type of active site, the randomness does not reach the unity ( $R \approx 0.98$  for  $N = 100$  and  $R \approx 0.86$  for  $N = 10$ ). The second source of heterogeneity comes from varying the fractions of different types of active sites. This leads to large variations in  $R$  as a function of  $N_1$  for the fixed total number of active sites. The third source of heterogeneity is due to the differences between chemical mechanisms  $R_1$  and  $R_2$ . This can be seen when we vary the transition rate  $a_1$  [Fig. 3(a)] or the transition rate  $a_2$  [Fig. 3(b)] for the fixed other parameters in the system. The advantage of our theoretical approach is that all these different sources of heterogeneity can be separated, fully quantified, and explained using microscopic arguments.

In addition, our theoretical method suggests that the analysis of experimental data might be used to determine the important microscopic properties of the single nanocatalysts. More specifically, we propose that by varying the degrees of catalytic activities (for example, by modifying temperatures or substrate concentrations)

and monitoring the changes in the randomness,<sup>15</sup> one could, in principle, determine the fractions of catalytic sites of different types. One can see from Eq. (21) that at the location when the randomness is minimal, we expect the fraction of the sites of the type  $R_1$  to be  $N_1/N \approx a_2/(a_1 + a_2)$  for the same number of intermediates in both chemical mechanisms. Analyzing experimental observations that exhibit such minimal randomness behavior can help to estimate the fractions of different types of sites, as suggested by Eq. (21).

The degree of stochastic fluctuations in the system also depends on the number of intermediate chemical states in the catalytic mechanisms, as shown in Fig. 4(a). The randomness parameter as a function of the number of intermediate chemical states  $M$  ( $M_1 = M_2 = M$ ) is presented there for the variable number of active sites  $N_1$ . In all situations, we observe a non-monotonic dependence. When  $M = 0$ , it corresponds to the single-step non-catalytic reactions, and the randomness here is  $R = 1$ . It is found also that the randomness is minimal (i.e., maximal degree of fluctuations) for  $M = 1$ , and then it approaches again the unity for  $M \rightarrow \infty$ . This behavior is similar to what was also observed in the homogeneous nanocatalyst system with only one type of site.<sup>31</sup>

Our theoretical approach provides a convenient way to explain these observations. For this purpose, we employ the chemical-kinetic scheme of effective states from Fig. 1(c). In the case where  $M = 0$ , the nanocatalyst is always in the effective catalytic state  $(N_1, N_2)$  since all states are one step away from making the product molecules. For this situation, Eq. (18) reduces to  $\tilde{F}_{N_1, N_2}(s) = \frac{1}{s + a_1 N_1 + a_2 N_2}$ , giving us

$$\langle T_{N_1, N_2} \rangle = \langle \tau \rangle_{N_1, N_2} = \frac{1}{a_1 N_1 + a_2 N_2} \quad (22)$$

and

$$\langle T_{N_1, N_2}^2 \rangle = \langle \tau_{N_1, N_2}^2 \rangle = \frac{2}{(a_1 N_1 + a_2 N_2)^2}. \quad (23)$$

Substituting these expressions into Eq. (18) eventually leads to  $R = 1$ . Another limiting case is  $M \rightarrow \infty$ , when it takes a very large number



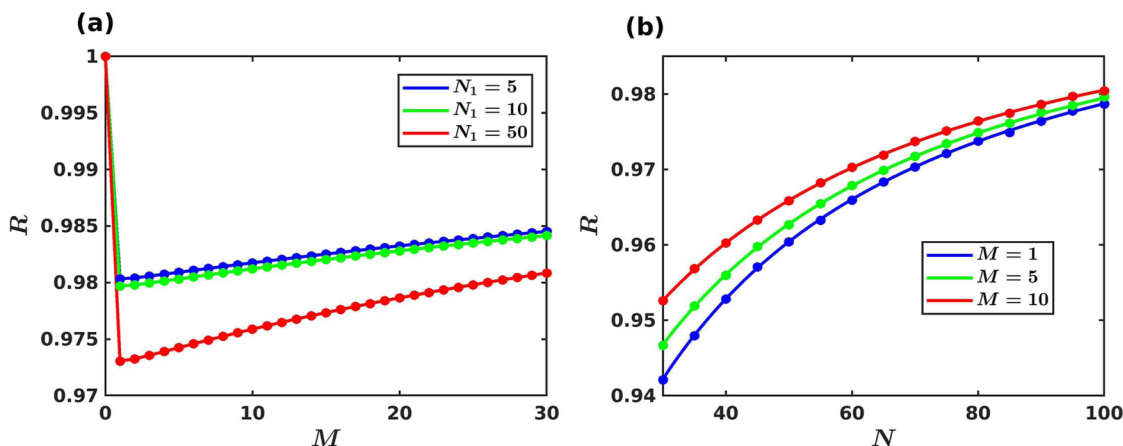


**FIG. 4.** Randomness parameter as a function of (a) the number of intermediate states  $M$  with different numbers of catalytic sites  $N_1$  and (b) the total number of active sites. The following parameters have been used in the calculations:  $a_1 = 2$ ,  $a_2 = 1$ , and  $N = 100$ . The curves are analytical predictions [using Eq. (18)], and the symbols are from Monte Carlo computer simulations.

of intermediate steps to complete the reaction. This means that the system preferentially starts in the effective state  $(0, 0)$  [see Fig. 1(c)], and this again leads to a minimal degree of fluctuations with  $R = 1$ . The case of  $M = 1$  corresponds to the situation when the system initiates mostly in the middle of the network of states, closer to the state  $(N_1/2, N_2/2)$ . However, from this state, multiple transitions in all directions are possible [see Fig. 1(c)], explaining the minimal randomness that corresponds to the largest possible stochasticity in the system. Increasing the parameter  $M$  pushes the system to start preferentially closer to the state  $(0, 0)$ , and this decreases the degree of stochastic fluctuations, explaining the trend of  $R \rightarrow 1$ .

Figure 4(b) shows the dependence of the randomness parameter on the total number of active sites. As expected, increasing

$N$  lowers the stochastic effects, and this leads to an increase in the randomness parameter  $R$ . In addition, one can see that the details of the chemical mechanisms (e.g., the number of intermediate states) become less relevant for larger numbers of active sites, and all curves for different values of  $M$  are converging [see Fig. 4(b)]. Furthermore, in agreement with our arguments presented earlier, the strongest fluctuations are observed for the case  $M = 1$  since in this case the system preferentially starts in the middle of the network of effective chemical states [Fig. 1(c)]. Increasing  $M$  shifts the location of the preferred initial state closer to the boundaries of the network of states, and this should increase the randomness parameter due to the lowering of the stochastic effects.

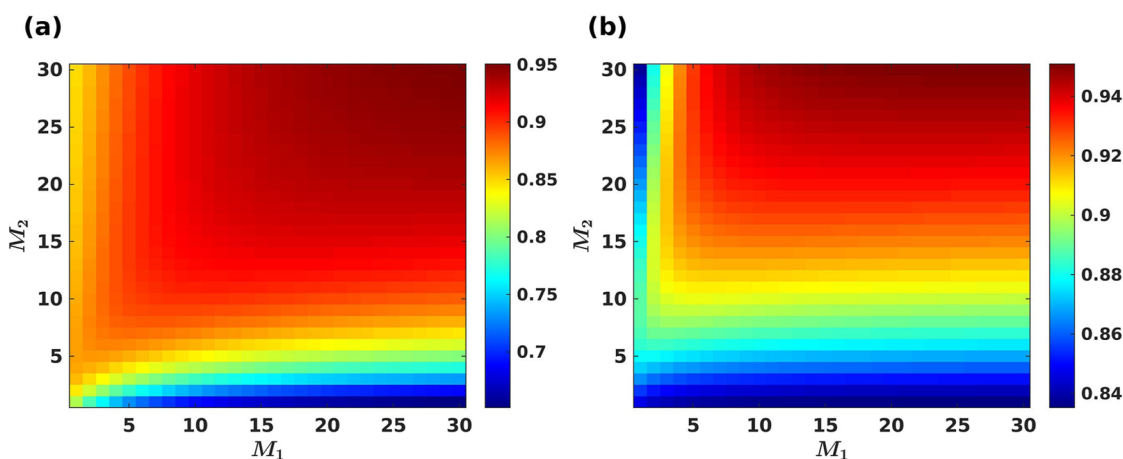


**FIG. 5.** Heat map representations of the randomness parameter [using Eq. (18)], as a function of the numbers of intermediate states  $M_1$  and  $M_2$  with the fixed total number of active sites  $N = 10$ , (a) for  $N_1 = 8$  and  $N_2 = 2$ , and (b) for  $N_1 = 2$  and  $N_2 = 8$ . The numbers of intermediate states are varied between 1 and 30. The following parameters have been used for calculations:  $a_1 = 2$  and  $a_2 = 8$ .

One of the sources of heterogeneity in the system that we have already identified is the variation in the mechanisms of chemical reactions at different active sites. In Fig. 3, we exhibited this effect by varying the catalytic efficiency of the sites by changing the corresponding transition rates  $a_1$  and  $a_2$ . Our theoretical approach also allows us to investigate another aspect of this phenomenon. One can modify the dynamics of catalyzed processes by varying the structure of the chemical mechanisms. More specifically, we can change the number of intermediate states  $M_1$  and  $M_2$  while keeping the same transition rates  $a_1$  and  $a_2$ . The results of our calculations for the randomness parameter with varying  $M_1$  and  $M_2$  are presented in Fig. 5. One can see dramatic variations in the degree of stochastic fluctuations in the system due to varying the chemical mechanisms on the active sites of the nanocatalyst. We predict that the largest fluctuations in the system occur when  $M_1$  or  $M_2$  is small, while the stochasticity decreases when both  $M_1$  and  $M_2$  are simultaneously large.

To illustrate the complexity of the behavior of the system when the chemical mechanisms are modified, in Fig. 6, we present the randomness parameter for the fixed values of the intermediate states  $M_2$  when  $M_1$  is varied. These graphs correspond to the cross-sections in Fig. 5(a). When the number of intermediate states for the mechanism  $R_2$  is large ( $M_2 = 28$ ), the system preferentially starts in the states that are close to the vertical set of states  $(n, 0)$  [see Fig. 1(c)]. The increase in the number of intermediate states  $M_1$  corresponds to shifting the initial state in the direction of the state  $(0, 0)$ . However, we know that the stochastic effects in this state are minimal. This explains the increase in the randomness parameter (blue curve in Fig. 6). The trend is the opposite when the number of intermediate states for the mechanism  $R_2$  is small ( $M_2 = 2$ ). In this case, the system preferentially starts in the bulk of the network of effective states [see Fig. 1(c)]. Then increasing  $M_1$  makes the contribution of the states of type  $R_1$  to the overall dynamics less important. This effectively decreases the number of active sites in the system, leading to larger stochastic effects and a lowering of the randomness parameter (red curve in Fig. 6).

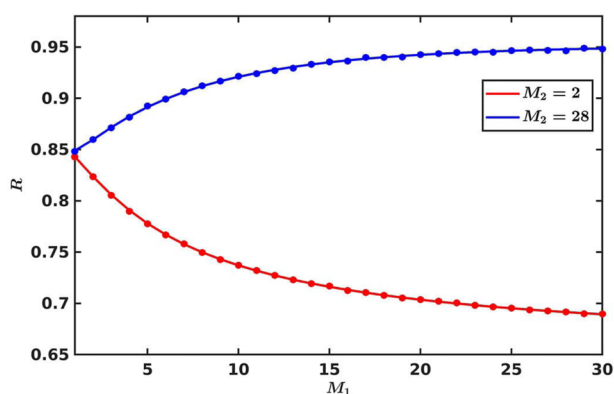


**FIG. 6.** The randomness parameter as a function of the number of intermediate states  $M_1$  for the fixed values of  $M_2$  for  $N_1 = 8$ ,  $N_2 = 2$ ,  $a_1 = 2$ , and  $a_2 = 8$ . The curves are analytical predictions [using Eq. (18)], and the symbols are from Monte Carlo computer simulations.

In addition to analytical calculations, we performed Monte Carlo computer simulations for the discrete-state stochastic model illustrated in Fig. 1(c). The standard kinetic Monte Carlo procedures have been followed, and only the large-time properties have been reported. The results of computer simulations are shown as symbols in Figs. 2–4 and 6. Error bars are typically smaller than the sizes of the symbols and are not shown. Excellent agreement between analytical calculations and computer simulations is observed in all cases.

#### IV. SUMMARY AND CONCLUSIONS

We theoretically investigated the role of heterogeneity in the dynamics of chemical processes that are taking place on single nanocatalysts. It is done by extending the discrete-state stochastic approach to account for various sources of heterogeneity by considering two different types of active sites with different chemical mechanisms. Our theoretical approach maps all processes in the system onto a 2D network of effective states that allows us to explicitly compute all dynamic properties in the system by utilizing forward and backward master equations methods. Analyzing mean reaction times, fluxes, and the randomness parameters, we identified three different sources of heterogeneity that influence the degree of stochastic fluctuations in the system: namely, the stochasticity of chemical reactions, the heterogeneity in the composition of active sites, and the variations in the chemical mechanisms at different active sites. It is also discussed how our theoretical method can be applied to real nanocatalyst systems to obtain important microscopic information on underlying processes. Therefore, using the presented analytical framework together with experimental observations on the dynamics of chemical reactions should significantly improve our understanding of molecular mechanisms of catalysis. Importantly, this means that heterogeneity can be used as a valuable *quantitative* tool for studies of the microscopic mechanisms of catalytic systems.

It is also important to critically analyze our theoretical method and to discuss future directions. Although our model gives a comprehensive analytical description of the molecular mechanism of chemical reactions on catalysts with different types of surface sites, there are several assumptions and simplifications that might affect the obtained results. In our analysis, we ignored the backward chemical transitions, and all transition rates for the given mechanism have been assumed to be the same. It has been argued that taking these effects into account will only change the quantitative nature of the results without affecting the physics. Computer simulations have been utilized to test this assumption, and no quantitative changes were observed (the results are not shown). We also assumed that all active sites are independent of each other, while there is recent experimental evidence that different sites on nanocatalysts might communicate with each other.<sup>9,36,37</sup> It will be interesting to explore how heterogeneity affects catalytic communications. In addition, it was assumed that the number of sites of different types remains constant in our model, while in real systems, the activities of catalytic sites might fluctuate over time due to surface dynamic restructuring on nanoparticles. This is a common situation in nanostructured and fluxional catalysts, i.e., in those systems with multiple inter-conversions between different configurations of catalysts. In addition, it will be important to extend our theoretical analysis to an

arbitrary number of different active sites, since this corresponds to a more realistic situation for catalytic systems. It will also be crucial to test experimentally our specific theoretical predictions.

## SUPPLEMENTARY MATERIAL

See the [supplementary material](#) for a complete description of the calculations of reaction times and stationary probabilities.

## ACKNOWLEDGMENTS

P.J. acknowledges IISER Pune for the fellowship. S.C. acknowledges the support from SERB, India (Grant No. CRG/2019/000515). A.B.K. acknowledges the support from the Welch Foundation (Grant No. C-1559), from the NSF (Grant Nos. CHE-1953453 and MCB-1941106), and from the Center for Theoretical Biological Physics sponsored by the NSF (Grant No. PHY-2019745).

## AUTHOR DECLARATIONS

### Conflict of Interest

The authors have no conflicts to disclose.

## Author Contributions

**Srabanti Chaudhury:** Conceptualization (equal); Data curation (equal); Formal analysis (equal); Funding acquisition (equal); Project administration (equal); Supervision (equal); Writing – original draft (equal); Writing – review & editing (equal). **Pankaj Jangid:** Formal analysis (equal); Investigation (equal); Project administration (equal); Validation (equal). **Anatoly B. Kolomeisky:** Conceptualization (equal); Funding acquisition (equal); Investigation (equal); Methodology (equal); Writing – review & editing (equal).

## DATA AVAILABILITY

The data that support the findings of this study are available within the article and its [supplementary material](#).

## REFERENCES

- <sup>1</sup>G. A. Somorjai and Y. Li, *Introduction to Surface Chemistry and Catalysis*, 2nd ed. (John Wiley and Sons, Chichester, UK, 2010).
- <sup>2</sup>J. R. Ross, *Heterogeneous Catalysis: Fundamentals and Applications* (Elsevier, 2011).
- <sup>3</sup>C. M. Friend and B. Xu, *Acc. Chem. Res.* **50**, 517 (2017).
- <sup>4</sup>D. Y. Murzin and T. Salmi, *Catalytic Kinetics* (Elsevier, 2005).
- <sup>5</sup>D. Y. Murzin, *Engineering Catalysis* (de Gruyter, 2020).
- <sup>6</sup>G. A. Somorjai, A. M. Contreras, M. Montano, and R. M. Rioux, *Proc. Natl. Acad. Sci. U. S. A.* **103**, 10577 (2006).

- <sup>7</sup>F. Tao, M. E. Grass, Y. Zhang, D. R. Butcher, J. R. Renzas, Z. Liu, J. Y. Chung, B. S. Mun, M. Salmeron, and G. A. Somorjai, *Science* **322**, 4932 (2008).
- <sup>8</sup>D. E. Makarov, *Single Molecule Science: Physical Principles and Models* (CRC Press, 2015).
- <sup>9</sup>P. Chen, X. Zhou, N. M. Andoy, K.-S. Han, E. Choudhary, N. Zou, G. Chen, and H. Shen, *Chem. Soc. Rev.* **43**, 1107 (2014).
- <sup>10</sup>W. Xu, J. S. Kong, Y.-T. E. Yeh, and P. Chen, *Nat. Mater.* **7**, 992–996 (2008).
- <sup>11</sup>F.-R. F. Fan and A. J. Bard, *Nano Lett.* **8**, 1746 (2008).
- <sup>12</sup>F.-R. F. Fan and A. J. Bard, *Science* **267**, 871–874 (1995).
- <sup>13</sup>C. Novo, A. M. Funston, and P. Mulvaney, *Nat. Nanotechnol.* **3**, 598–602 (2008).
- <sup>14</sup>J. B. Sambur and P. Chen, *Annu. Rev. Phys. Chem.* **65**, 395 (2014).
- <sup>15</sup>W. Xu, J. S. Kong, and P. Chen, *Phys. Chem. Chem. Phys.* **11**, 2767 (2009).
- <sup>16</sup>H. P. Lu, L. Xun, and X. S. Xie, *Science* **282**, 1877–1882 (1998).
- <sup>17</sup>B. P. English, W. Min, A. M. van Oijen, K. T. Lee, G. Luo, H. Sun, B. J. Cherayil, S. C. Kou, and X. S. Xie, *Nat. Chem. Biol.* **2**, 87 (2006).
- <sup>18</sup>M. B. J. Roeffaers, B. F. Sels, H. Uji-i, F. C. De Schryver, P. A. Jacobs, D. E. De Vos, and J. Hofkens, *Nature* **439**, 572–575 (2006).
- <sup>19</sup>K. Naito, T. Tachikawa, M. Fujitsuka, and T. Majima, *J. Phys. Chem. C* **112**, 1048 (2008).
- <sup>20</sup>M. A. Ochoa, P. Chen, and R. F. Loring, *J. Phys. Chem. C* **117**, 19074 (2013).
- <sup>21</sup>X. Zhou, N. M. Andoy, G. Liu, E. Choudhary, K.-S. Han, H. Shen, and P. Chen, *Nat. Nanotechnol.* **7**, 237 (2012).
- <sup>22</sup>P. L. Hansen, J. B. Wagner, S. Helveg, J. R. Rostrup-Nielsen, B. S. Clausen, and H. Topsøe, *Science* **295**, 2053 (2002).
- <sup>23</sup>Z. L. Wang, *Adv. Mater.* **15**, 1497 (2003).
- <sup>24</sup>X. Zhou, W. Xu, G. Liu, D. Panda, and P. Chen, *J. Am. Chem. Soc.* **132**, 138–146 (2010).
- <sup>25</sup>K. S. Han, G. Liu, X. Zhou, R. E. Medina, and P. Chen, *Nano Lett.* **12**, 1253–1259 (2012).
- <sup>26</sup>Y. Zhang, P. Song, T. Chen, X. Liu, T. Chen, Z. Wu, Y. Wang, J. Xie, and W. Xu, *Proc. Natl. Acad. Sci. U. S. A.* **115**, 10588 (2018).
- <sup>27</sup>W. Xu, J. S. Kong, and P. Chen, *J. Phys. Chem. C* **113**, 2393 (2009).
- <sup>28</sup>A. Das and S. Chaudhury, *Chem. Phys. Lett.* **641**, 193 (2015).
- <sup>29</sup>D. Singh and S. Chaudhury, *Phys. Chem. Chem. Phys.* **19**, 8889 (2017).
- <sup>30</sup>S. Chaudhury, D. Singh, and A. B. Kolomeisky, *J. Phys. Chem. Lett.* **11**, 2330 (2020).
- <sup>31</sup>B. Punia, S. Chaudhury, and A. B. Kolomeisky, *J. Phys. Chem. Lett.* **12**, 11802 (2021).
- <sup>32</sup>T. Tachikawa, S. Yamashita, and T. Majima, *J. Am. Chem. Soc.* **133**, 7197 (2011).
- <sup>33</sup>T. Chen, S. Chen, Y. Zhang, Y. Qi, Y. Zhao, W. Xu, and J. Zeng, *Angew. Chem.* **128**, 1871 (2016); **55**, 1839 (2016).
- <sup>34</sup>K. Rossi, G. G. Asara, and F. Baletto, *ChemPhysChem* **20**, 3037 (2019).
- <sup>35</sup>K. Rossi, G. G. Asara, and F. Baletto, *ACS Catal.* **10**, 3911 (2020).
- <sup>36</sup>N. Zou, X. Zhou, G. Chen, N. M. Andoy, W. Jung, G. Liu, and P. Chen, *Nat. Chem.* **10**, 607 (2018).
- <sup>37</sup>B. Punia, S. Chaudhury, and A. B. Kolomeisky, *Proc. Natl. Acad. Sci. U. S. A.* **119**, e2115135119 (2022).
- <sup>38</sup>A. B. Kolomeisky, *Motor Proteins and Molecular Motors* (CRC Press, 2015).
- <sup>39</sup>R. Metzler, S. Redner, and G. Oshanin, *First-Passage Phenomena and Their Applications* (World Scientific, 2014), Vol. 35.
- <sup>40</sup>S. Redner, *A Guide to First-Passage Processes* (Cambridge University Press, 2001).
- <sup>41</sup>N. G. Van Kampen, *Stochastic Processes in Physics and Chemistry* (Elsevier, 1992), Vol. 1.
- <sup>42</sup>S. Yang, J. Cao, R. J. Silbey, and J. Sung, *Biophys. J.* **101**, 519 (2011).